ATLAS PUB Note

ATL-PHYS-PUB-2021-021

9th June 2021

Search for non-resonant signatures of extra dimensions in high-mass dilepton final states in 139 fb^{-1} of pp collisions at $\sqrt{s}$=13 TeV using the ATLAS detector

The ATLAS Collaboration

A reinterpretation of the search for non-resonant phenomena in dielectron and dimuon final states is presented to search for the ADD model of large extra spatial dimensions. The data analyzed was collected by the ATLAS detector, between 2015 and 2018, and produced by LHC proton-proton collisions at a centre-of-mass energy $\sqrt{s}$ = 13 TeV. This corresponds to a total integrated luminosity of 139 fb^{-1}. The dilepton invariant mass spectra are used as the discriminating variables. No significant deviations from the Standard Model expectation are observed. Lower limits are set on the string scale M_S between 6.6 TeV and 6.4 TeV at the 95% confidence level for the electron and muon channel, respectively, in the GRW convention of the ADD model.

© 2021 CERN for the benefit of the ATLAS Collaboration.
Reproduction of this article or parts of it is allowed as specified in the CC-BY-4.0 license.

1 Introduction

Many theories beyond the Standard Model (SM) predict new phenomena which give rise to dilepton final states (where the leptons considered in this analysis are electrons or muons), such as new resonances or excesses at large invariant mass. These theories have been searched for using the ATLAS detector at the Large Hadron Collider (LHC) in both Run 1, operating at centre-of-mass energy $\sqrt{s}$ = 7 TeV and 8 TeV, and Run 2, operating at $\sqrt{s}$ = 13 TeV. The Run 2 data was collected between 2015 and 2018 and was produced by LHC proton-proton collisions at $\sqrt{s}$ = 13 TeV. It corresponds to an integrated luminosity of 139 fb^{-1}. The latest ATLAS Run 2 dilepton resonant search for bosons producing narrow resonances is presented in Ref. [1] and a complementary search for new phenomena that appear as broad deviations from the SM in the invariant mass distribution of the two leptons, specifically interpreted in terms of contact interactions (CI) is reported in Ref. [2]. This note presents a reinterpretation of this non-resonant analysis to set limits on the existence of large extra dimensions (LED), which would also result in a broad excess of events at large invariant mass [3]. In the CI paper, and therefore in the reinterpretation presented here, the SM background is estimated by fitting a parametric-function to data in the low-mass region and extrapolating to the high-mass region. This technique succeeds the method used in Run 1 and early Run 2 dilepton searches which used Monte Carlo simulations to estimate the backgrounds [4–7]. Moreover, contrary to the Run 1 ATLAS search for non-resonant signals in dilepton final states, at $\sqrt{s}$=8 TeV, this search is performed in a single-bin high mass signal region [8]. This present analysis uses a frequentist statistical approach, which removes the dependence on signal priors, rather than the Bayesian method used in Run 1 and early Run 2 searches.

2 Theoretical models

Several models predict deviations from the SM in the dilepton mass spectrum. Models which seek to address the vast hierarchy between the electroweak (EW) and Planck scales can predict resonant deviations, or non-resonant deviations in the dilepton invariant mass distribution. The solution considered in the current note is proposed by Arkani-Hamed, Dimopoulos and Dvali (ADD) [3]. In this model, gravity is able to propagate into large flat extra spatial dimensions, thereby diluting its apparent effect in the usual 3+1 spacetime dimensions. The flat n extra dimensions are of common size R ($\sim$1 μm - 1 mm for $n = 2$) and are compactified on an n-dimensional torus. The fundamental Planck scale in $(4 + n)$-dimensions, M_D, is related to the Planck scale, M_{Pl}, by Gauss's law $M_{\mathrm{Pl}}^2 \sim M_{\mathrm{D}}^{n+2} R^n$. Thus for sufficiently large volumes ($\propto R^{\mathrm{n}}$), M_{D} can be in the TeV range. In this model, gravitons propagate in the bulk of $(4 + n)$-dimensional spacetime, whereas SM particles and their interactions are confined to the four-dimensional manifold. Compactifying the extra dimensions in ADD theory leads to a tower of Kaluza-Klein (KK) graviton modes with a mass spacing inversely proportional to R. Values of M_{D} at the TeV scale imply very small mass differences between KK modes and thus produce an essentially continuous mass spectrum. The production of dileptons via virtual KK graviton exchange involves a sum over many KK modes which needs to be cut off at some value. In this note, the ultraviolet cutoff is chosen, for consistency with previous searches, to be the string scale, M_{S}. This sets the context in which the results of this search are reinterpreted. The string scale, M_{S}, is related to M_{D} via the Gamma function, Γ as shown in Equation 1 [9].

$$M_{\mathrm{S}} = 2\sqrt{\pi}\left[\Gamma\left(\frac{n}{2}\right)\right]^{1/(n+2)} M_{\mathrm{D}} \tag{1}$$

The total cross-section, σ_{tot}, for dilepton production in the presence of large extra dimensions can be expressed by Equation 2. This has three terms, a term for the SM DY cross-section, σ_{DY}, the interference of the KK gravitons with the SM, and one which describes the purely gravitational KK interactions. The latter two terms are governed by the M_{S}-independent functions F_{int} and F_{grav} respectively.

$$\sigma_{\text{tot}} = \sigma_{\text{DY}} + \mathscr{F}\frac{F_{\text{int}}}{M_{\text{S}}^4} + \mathscr{F}^2\frac{F_{\text{G}}}{M_{\text{S}}^8} \tag{2}$$

The strength of the interaction is characterized by $\mathscr{F}/M_{\text{S}}^4$, where the dimensionless parameter $\mathscr{F}$ varies in the different calculations provided by Giudice-Rattazzi-Wells (GRW) [10], Hewett [11] and Han-Lykken-Zhang (HLZ) [12].

The different conventions are:

$$\mathscr{F} = 1 \quad \text{(GRW)},$$

$$\mathscr{F} = \frac{2\lambda}{\pi} = \frac{\pm 2}{\pi} \quad \text{(Hewett)},$$

$$\mathscr{F} = \log\left(\frac{M_{\text{S}}^2}{\hat{s}}\right) \quad \text{for } n = 2 \quad \text{(HLZ)},$$

$$\mathscr{F} = \frac{2}{n-2} \quad \text{for } n > 2 \quad \text{(HLZ)}.$$

In the Hewett formalism, $\lambda = \pm 1$ is introduced to allow for constructive or destructive interference with the DY process. The Hewett $\lambda = -1$ results can not be scaled directly from the GRW convention. Therefore, in this analysis no limits are set for this convention. The graviton can be produced by quark-anti-quark annihilation, or can be gluon initiated, as illustrated in Figure 1. The fraction of events produced by each process is dependent on M_{S}.

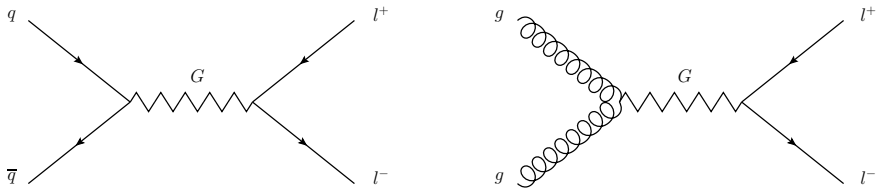

Figure 1: Feynman diagrams showing quark-anti-quark and gluon initiated graviton production and subsequent decay to two leptons.

Previous searches for evidence of ADD-model extra dimensions via virtual KK graviton exchange have been performed at electron-positron [13], electron-proton [14], and proton-antiproton colliders [15]. Searches have also been performed at the LHC by the ATLAS and CMS Collaborations [5, 16]. The most stringent ATLAS results were set by the Run 1 search using the combination of the dielectron and dimuon channels using 20 fb^{-1} of pp collision data at $\sqrt{s} = 8$ TeV [8]. This analysis sets lower limits on M_{S} at 95% C.L. of 4.2 TeV and 4.0 TeV for $1/M_{\text{S}}^4$ and $1/M_{\text{S}}^8$ priors respectively, in the GRW formalism. The CMS Collaboration have published a search for large extra dimensions using their full Run 2 dilepton dataset [17]. The CMS observed (expected) limits, in the GRW convention, with a NNLO correction factor of 1.0, are 6.7 (6.9) TeV in the dielectron channel, 7.0 (7.1) TeV in the dimuon channel, and 7.3 (7.5) TeV for the combination [17]. In constrast to this analysis, CMS search performs a multi-bin analysis and uses a Monte-Carlo based method to estimate the expected backgrounds. It is possible to search for ADD-model

extra dimensions via graviton emission, such searches have been performed by the ATLAS and CMS collaborations, in the mono-jet and mono-photon channels [18–21].

3 Data and Monte Carlo samples

The data used in this search are the same as those used in the resonant and non-resonant dilepton searches which analyse the full Run 2 dataset [1, 2]. This data was collected at the LHC between 2015 and 2018 from pp collisions at $\sqrt{s}$ = 13 TeV. The total integrated luminosity corresponds to 139 fb^{-1}, collected during LHC stable beam conditions, when all detector systems were operating correctly and all quality requirements were satisified. The uncertainty in the combined 2015-2018 integrated luminosity is 1.7% [22].

ADD signal samples were generated at next-to-leading order (NLO) using Sherpa with CT10 for six values of M_S, ranging from 3000 GeV to 8000 GeV [23, 24]. These samples include a DY component as well as signal. Therefore, to obtain signal-only samples, a DY sample is generated and subtracted from the signal samples.

The dominant background contribution arises from the DY process. Other backgrounds, which contribute a smaller fraction, originate from top-quark and diboson (WW, WZ, ZZ) production. In the case of the dielectron channel, multi-jet and W+jets processes contribute due to the misidentification of jets as electrons. Monte-Carlo generated, simulated and reconstructed samples are used to validate and optimise the data-driven background estimation, rather than used to ascertain the background. The Monte Carlo files are described in detail in Ref. [2]. The multi-jet and W+jets background processes are estimated from the data using the matrix method as described in Ref. [25].

The background in this analysis is estimated by fitting a parametric background-model function to the data in a low mass control region (CR), and extrapolating to the higher-mass single-bin signal region (SR). The fits are implemented using the RooFit framework [26]. The background fit function is normalised in the CR using the number of events in the CR in data (or simulation where applicable), where it is assumed that the CR is completely dominated by background events.

The choice of the CR and SR boundaries is described in detail in Ref. [2] and summarised in Table 1. The function used to fit the background is Equation 3, in which $x = \frac{m_{ll}}{\sqrt{s}}$, where m_{ll} describes the dilepton invariant mass distribution [1].

$$f_b(m_{ll}) = f_{BW,Z}(m_{ll}) \cdot (1 - x^c)^b x^{\sum_{i=0}^{3} p_i log(x)^i} \tag{3}$$

The first term, $f_{BW,Z}(m_{ll})$ is a non-relativistic Breit-Wigner function with m_Z = 91.1876 GeV and Γ_Z = 2.4952 GeV [2]. The function $f_b(m_{ll})$ is treated as a probability density function in the fits performed in the CR.

4 Control and search regions

Different choices of CR and SR were considered in the non-resonant CI search in order to maximise the expected sensitivity for each lepton channel and for different choices of the CI model parameters [2]. For this extra dimensional non-resonant search the SRs optimised for the destructive CI signal give the best

expected limits. The CR and SR ranges (in units of GeV) used in this analysis are stated in Table 1, where the upper boundary on the signal region (SR_{max}) is 6 TeV.

Channel	CR_{min}	CR_{max}	SR_{min}	SR_{max}
ee	310	1450	2770	6000
$\mu\mu$	320	1250	2570	6000

Table 1: Control region (CR) and signal region (SR) ranges (in units of GeV).

5 Event selection

The event selection is the same as is implemented in the resonant dilepton search and the non-resonant search for contact interactions. Both the object reconstruction and event selection are described in detail in Ref. [1] and the electron and muon selections are summarised in Table 2.

Dilepton candidates are selected in the data and simulated events by requiring at least one pair of reconstructed same-flavour lepton candidates (electrons or muons) and at least one reconstructed pp interaction vertex, with the primary vertex defined as the one with the highest sum of track transverse momenta (p_T) squared.

If an event contains more than two leptons, then the two leptons with the largest rransverse energy, E_T (p_T), in the electron (muon) channel are selected to form the dilepton pair. The muons within a selected pair are required to have opposite electric charge. Because of the higher probability of charge misidentification for high E_T electrons, the opposite-charge requirement is not applied for electron pairs. If an event contains both a dielectron and a dimuon pair, the dielectron pair is selected because of the better resolution and higher efficiency for electrons. To avoid the Z boson peak region, which cannot be described by the same parameterisation as the high-mass part of the dilepton distributions, the reconstructed mass of the dilepton system after the full analysis selection, m_{ll}, is required to be above 130 GeV.

Electron selection	**Muon selection**
Trigger	
2 e with E_T > 12 - 24 GeV [1]	1 μ with p_T > 50 GeV
Acceptance	
$\|\eta\|$ < 2.47 excluding region 1.37 < $\|\eta\|$ < 1.52 E_T > 30 GeV	$\|\eta\|$ < 2.5 excluding region 1.01 < $\|\eta\|$ < 1.10 p_T > 30 GeV
Primary vertex (PV)	
Track from PV Longitudinal displacement near PV Transverse displacement near PV	
Quality selection	
Medium working point likelihood criteria [27] Track isolation (variable cone size) Calorimeter isolation (E_T dependent, in cone ΔR = 0.2)	High-p_T working point [28] Track isolation (variable cone size) ($\frac{q}{p}$) requirement

Table 2: Electron (left) and muon (right) selection criteria.

6 Event yields

The dielectron and dimuon invariant mass (m_{ll}) distributions for data passing the full analysis selection and for the background expectation, as published in Ref. [2] are shown in Figure 2, together with example ADD signals. In these histograms, all of the simulation-based background contributions are scaled by their respective cross-sections and summed to obtain the total simulated background m_{ll} distribution. Note that these MC simulated backgrounds are not used for limit setting. The dielectron and dimuon invariant mass distributions showing the data-driven background distribution, the data and potential signal events in the control, gap and the signal region, are displayed in Figure 3 and Figure 4, respectively. The expected signal event yields in the signal regions are stated in Table 4 for the dielectron channel and in Table 5 for the dimuon channel.

Two events were observed in the dielectron signal region and one in the dimuon signal region. The highest reconstructed invariant mass of lepton pairs is m_{ee} = 4.06 TeV in the dielectron and $m_{\mu\mu}$ = 2.75 TeV in the dimuon channel. No clear excess of events above the SM is observed, significances and discrepancies from data are quantified and presented in Table 3 [2].

The background only and predicted number of signal events in the signal region are used in a single-bin counting approach, explained in Ref. [2], to set limits on the scale of the large extra dimensions M_S. These are presented Section 8.

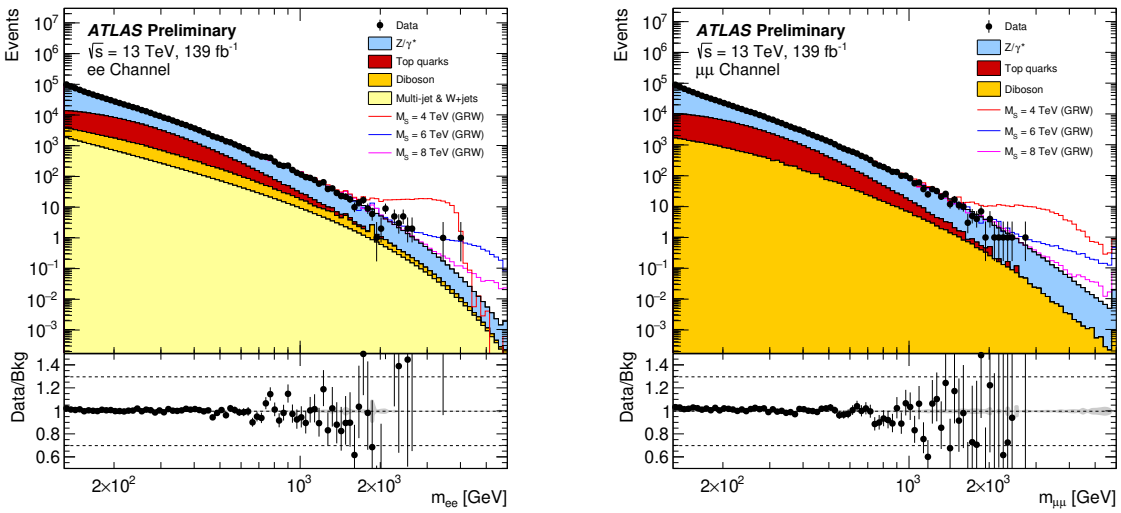

Figure 2: Invariant mass distribution for the data, the MC simulated backgrounds (identical to those in Ref. [2]), and the GRW ADD large extra dimensional model signal events for the dielectron (left) and dimuon (right) channels.

7 Systematic uncertainties

Uncertainties in this analysis orginate from fluctuations in the expected background and signal in the SR. In this fit-and-extrapolate approach, the dominant uncertainty in the expected background is due to statistical fluctuations in the CR affecting the extrapolation into the SR. Theoretical uncertainties can also alter the background estimation.

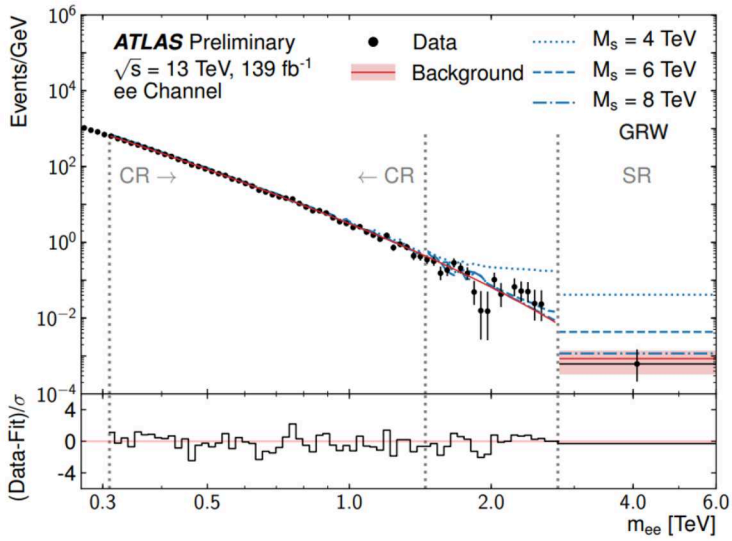

Figure 3: Dielectron invariant mass distribution for the data-driven background fit (solid line), the data (points), and the signal events (dashed lines) for several values of M_S in the GRW large extra-dimensional model. The control (CR), gap and signal region (SR) are also shown. The shaded region indicates the uncertainty on the background estimation in the SR and the lower insert presents a measure of the goodness of fit, the ratio of the (data-fit)/σ per bin.

Channel	Data	Background	Significance
ee	2	3.1 ± 1.1	-0.72
$\mu\mu$	1	1.4 ± 0.9	-0.58

Table 3: The dielectron and dimuon event yields, the expected background and the respective significance in the signal region. The p-value of each observation is defined as the probability, given the background-only hypothesis, of an observation at least as large as that seen in the data. The significance is the Gaussian cumulative density function of the p-value, and negative significances correspond to deficits [2].

Analogously to the non-resonant search for contact interactions, the systematic uncertainties which are estimated to have a non-negligible impact on the expected cross-section limit are considered as nuisance parameters in the statistical interpretation and include both the theoretical and experimental effects on the total background and experimental effects on the signal [2].

The expected number of ADD signal events in the SR is affected by experimental and theoretical uncertainties. The signal yield is obtained by integrating the simulated signal in the single-bin SR. This calculation is performed for all theoretical and experimental systematic variations of the signal. The uncertainty in the signal yield is obtained from the sum in quadrature of the differences between the yields obtained in all variations and the nominal yield.

As in the latest ATLAS non-resonant CI search [2], the experimental signal yield uncertainty is assumed to be the same as for the NLO DY in the signal region. Therefore, up and down variations of DY MC templates are used to calculate the uncertainty on the ADD signal. The uncertainties are 8.4% for the dielectron channel and 26.7% for the dimuon channel.

The theoretical uncertainty is evaluated from the difference between the number of events in the SR for various variations of PDF eigenvectors and a K-factor-corrected default PDF set. The uncertainty from the PDFs on the signal yields ranges between 10% at M_S = 3 TeV to 20% at M_S = 8 TeV.

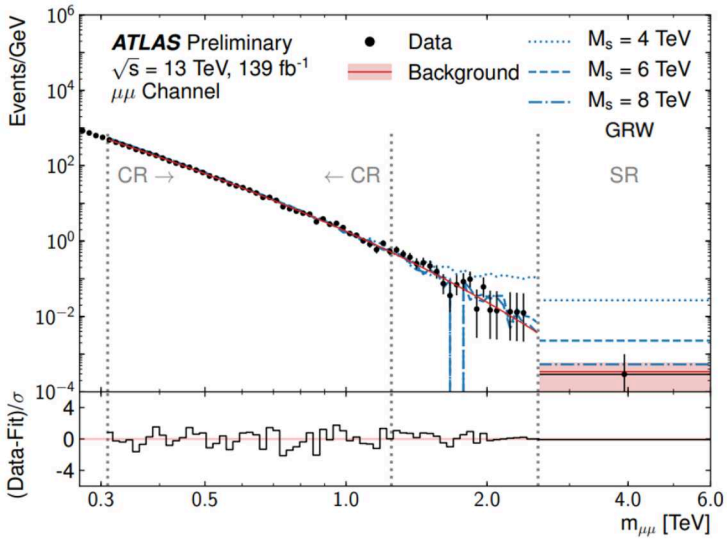

Figure 4: Dimuon invariant mass distribution for the data-driven background fit (solid line), the data (points), and the signal events (dashed lines) for several values of M_S in the GRW large extra-dimensional model. The control (CR), gap and signal region (SR) are also shown. The shaded region indicates the uncertainty on the background estimation in the SR and the lower insert presents a measure of the goodness of fit, the ratio of the (data-fit)/σ per bin.

ee Channel	
String Scale, M_S (GeV)	N_{sig}^{SR}
3000	126.1
4000	139.8
5000	40.5
6000	11.6
7000	3.3
8000	1.1

Table 4: Predicted number of dielectron signal events in the signal region (N_{sig}^{SR}) for different large extra-dimensional string scales M_S for the GRW convention.

8 Statistical analysis

A frequentist approach is used. The statistical analysis is described in detail in Ref. [2].

8.1 Extracting limits from the number of events observed

In order to set lower mass limits on M_S, the statistical framework used in the analysis requires a continuous function relating M_S to the number of (reweighted) signal events in the signal region. Only six graviton samples are generated. For these samples the number of signal events above the DY background can be determined via subtraction of the DY from the dedicated generated sample. To translate between the number of events observed and the corresponding value of M_S, an exponential interpolation is made between the number of signal events for the six generated M_S values using a morphing procedure.

$\mu\mu$ Channel	
String Scale, M_S (GeV)	N_{sig}^{SR}
3000	232.3
4000	98.9
5000	25.8
6000	6.9
7000	2.1
8000	0.65

Table 5: Predicted number of dimuon signal events in the signal region (N_{sig}^{SR}) for different large extra-dimensional string scales M_S for the GRW convention.

The difference in SR event yield between the 6 TeV template and morphed histogram is below 0.2% for the electron channel and 7% in the muon channel. This effect is smaller than the signal template statistical uncertainty and was deemed to be negligble and so not included in the limit setting.

8.2 Limit setting

The ADD cross-section is described by the second two terms in Equation 2, the first being the DY cross-section. The signal cross-section has two components, an interference and a pure graviton term. Limits on M_S are set in the GRW convention, for which $\mathscr{F} = 1$ in Equation 2. The number of signal events in the SR predicted by this cross-section, with $\mathscr{F} = 1$, and the number of expected background events in the SR are converted into a limit on M_S using the RooStats Frequentist Calculator [29]. The ADD signal samples are generated in the GRW convention, in the appropriate mixture of the interference ($\frac{F_{\text{int}}}{M_S^4}$) and graviton ($\frac{F_G}{M_S^8}$) terms. It is not possible to directly convert the number of events predicted in the GRW convention to that predicted in the Hewett and HLZ conventions. This would require separating the number of events predicted by the interference and graviton terms in the GRW samples, and then scaling these numbers by $\mathscr{F}$ and $\mathscr{F}^2$, respectively. Therefore, to convert the limits to other conventions, two cases are considered: one where $Y = \mathscr{F}$ in Equation 4, and the other where $Y = \mathscr{F}^2$, where the values of $\mathscr{F}$ are described in Section 2. The true lower mass limit, at the 95% confidence level, lies between these two values, which differ by less than or equal to 0.7 TeV for all cases, which are displayed in Table 6. Figure 5 and Figure 6 show the limits on M_S for scaling by $\mathscr{F}^2$ for the electron and muon channel respectively.

$$\sigma_{\text{ADD}} = Y\left(\frac{F_{\text{int}}}{M_S^4} + \frac{F_G}{M_S^8}\right) \tag{4}$$

9 Conclusion

This note presents the first limits set by the ATLAS Collaboration on the ADD model in dilepton final states using Run 2 data. The dataset analysed was collected by the ATLAS detector at the LHC with a pp collision centre-of-mass energy $\sqrt{s}$ = 13 TeV, recorded between 2015 and 2018 and corresponds to a total luminosity of 139 fb^{-1}. No significant deviations from the Standard Model predictions are observed and lower limits, at the 95% confidence level, are set on the scale of large extra dimensions, M_S, of 6.6 TeV and 6.4 TeV in the dielectron and dimuon channel respectively, in the GRW convention.

Channel	Cross Section Scaling	GRW	Hewett	HLZ				
			$\lambda = +1$	$n = 3$	$n = 4$	$n = 5$	$n = 6$	$n = 7$
Exp: ee	$\mathcal{F}$	6.5	6.2	7.0	6.5	6.2	6.0	5.8
Obs: ee		6.6	6.2	7.1	6.6	6.2	6.0	5.8
Exp: ee	$\mathcal{F}^2$	6.5	5.8	7.5	6.5	5.9	5.4	5.1
Obs: ee		6.6	5.9	7.6	6.6	5.9	5.5	5.1
Exp: μμ	$\mathcal{F}$	6.3	5.9	6.8	6.3	6.0	5.7	5.6
Obs: μμ		6.4	6.0	6.9	6.4	6.0	5.8	5.6
Exp: μμ	$\mathcal{F}^2$	6.3	5.6	7.3	6.3	5.7	5.2	4.9
Obs: μμ		6.4	5.7	7.4	6.4	5.7	5.3	5.0

Table 6: Lower limits, at 95% confidence level, on M_S in TeV for the ADD large extra dimensional model in the dielectron and dimuon channel for different model conventions.

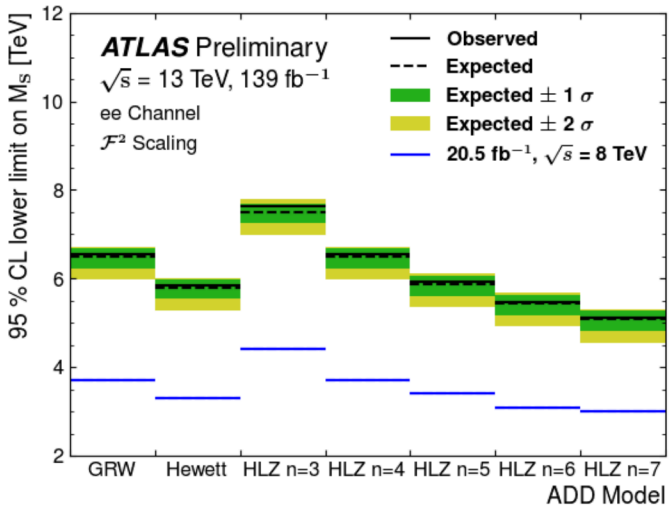

Figure 5: Lower limits, at 95% confidence level, on M_S in TeV for the ADD large extra dimensional model in the dielectron channel for different model conventions, scaling the cross section by $\mathcal{F}^2$.

References

[1] ATLAS Collaboration, *Search for high-mass dilepton resonances using 139 fb^{-1} of pp collision data collected at $\sqrt{s}$ =13 TeV with the ATLAS detector*, Phys. Lett. B **796** (2019) 68, arXiv: 1903.06248 (cit. on pp. 2, 4, 5).

[2] ATLAS Collaboration, *Search for new non-resonant phenomena in high-mass dilepton final states with the ATLAS detector*, JHEP **11** (2020) 05, arXiv: 2006.12946 (cit. on pp. 2, 4, 6–8).

[3] N. Arkani–Hamed, S. Dimopoulos and G. Dvali, *The hierarchy problem and new dimensions at a millimeter*, Phys. Lett. B **429** (1998) 263, arXiv: hep-ph/9803315 (cit. on p. 2).

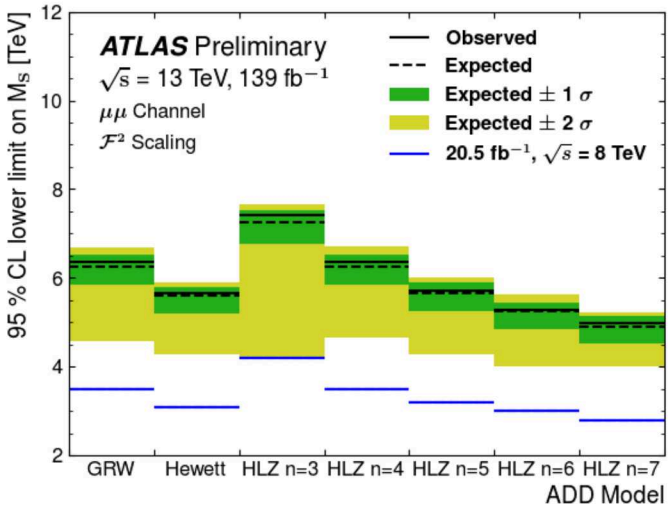

Figure 6: Lower limits, at 95% confidence level, on M_S in TeV for the ADD large extra dimensional model in the dimuon channel for different model conventions, scaling the cross section by $\mathscr{F}^2$.

[4] ATLAS Collaboration, *Search for high-mass resonances decaying to dilepton final states in pp collisions at $\sqrt{s}$ = 7 TeV with the ATLAS detector*, JHEP **11** (2012) 138, arXiv: 1209.2535 (cit. on p. 2).

[5] ATLAS Collaboration, *Search for contact interactions and large extra dimensions in dilepton events from pp collisions at $\sqrt{s}$ = 7 TeV with the ATLAS detector*, Phys. Rev. D **87** (2013) 015010, arXiv: 1211.1150 (cit. on pp. 2, 3).

[6] ATLAS Collaboration, *Search for high-mass new phenomena in the dilepton final state using proton–proton collisions at $\sqrt{s}$ = 13 TeV with the ATLAS detector*, Phys. Lett. B **761** (2016) 372, arXiv: 1607.03669 (cit. on p. 2).

[7] ATLAS Collaboration, *Search for new high-mass phenomena in the dilepton final state using 36 fb^{-1} of proton-proton collision data at $\sqrt{s}$ = 13 TeV with the ATLAS detector*, JHEP **10** (2017) 182, arXiv: 1707.02424 (cit. on p. 2).

[8] ATLAS Collaboration, *Search for contact interactions and large extra dimensions in the dilepton channel using proton–proton collisions at $\sqrt{s}$ = 8 TeV with the ATLAS detector*, Eur. Phys. J. C **74** (2014) 3134, arXiv: 1407.2410 (cit. on pp. 2, 3).

[9] T. Gleisberg et al., *Helicity formalism for spin-2 particles*, JHEP **09** (2003) 001, arXiv: hep-ph/0306182 (cit. on p. 2).

[10] G. F. Giudice, R. Rattazzi and J. D. Wells, *Quantum gravity and extra dimensions at high-energy colliders*, Nucl. Phys. B **544** (1999) 3, arXiv: hep-ph/9811291 (cit. on p. 3).

[11] J. L. Hewett, *Indirect Collider Signals for Extra Dimensions*, Phys. Rev. Lett. **82** (1999) 4765, arXiv: hep-ph/9811356 (cit. on p. 3).

[12] T. Han, J. D. Lykken and R.-J. Zhang, *Kaluza-Klein states from large extra dimensions*, Phys. Rev. D **59** (1999) 105006, arXiv: hep-ph/9811350 (cit. on p. 3).

[13] OPAL Collaboration, *Multi-photon production in ee collisions at* $\sqrt{s} = 181 - 209$ *GeV*, Eur. Phys. J. C **26** (2003) 331, arXiv: hep-ex/0210016 (cit. on p. 3).

[14] ZEUS Collaboration, *Search for contact interactions, large extra dimensions and finite quark radius in ep collisions at HERA*, Phys. Lett. B **591** (2004) 23, arXiv: hep-ex/0401009 (cit. on p. 3).

[15] D0 Collaboration, *Measurement of Dijet Angular Distributions at* $\sqrt{s} = 1.96$ TeV *and Searches for Quark Compositeness and Extra Spatial Dimensions*, Phys. Rev. Lett. **103** (2009) 191803, arXiv: 0906.4819 (cit. on p. 3).

[16] CMS Collaboration, *Search for contact interactions in* $\mu^+\mu^-$ *events in pp collisions at* $\sqrt{s} = 7$ *TeV*, Phys. Rev. D **87** (2013) 032001, arXiv: 1212.4563 (cit. on p. 3).

[17] CMS Collaboration, *Search for resonant and nonresonant new phenomena in high-mass dilepton final states at* $\sqrt{s} = 13$ *TeV*, (2021), arXiv: 2103.02708 (cit. on p. 3).

[18] ATLAS Collaboration, *Search for new phenomena in events with an energetic jet and missing transverse momentum in pp collisions at* $\sqrt{s} = 13$ *TeV with the ATLAS detector*, 2021, arXiv: 2102.10874 (cit. on p. 4).

[19] CMS Collaboration, *Search for new particles in events with energetic jets and large missing transverse momentum in proton-proton collisions at* $\sqrt{s}$*=13 TeV*, CMS-PAS-EXO-20-004, 2021, URL: https://cds.cern.ch/record/2771676 (cit. on p. 4).

[20] ATLAS Collaboration, *Search for new phenomena in events with a photon and missing transverse momentum in pp collisions at* $\sqrt{s} = 13$ *TeV with the ATLAS detector*, JHEP **06** (2016) 59, arXiv: 1604.01306 (cit. on p. 4).

[21] CMS Collaboration, *Search for new physics in final states with a single photon and missing transverse momentum in proton-proton collisions at* $\sqrt{s} = 13$ *TeV*, JHEP **02** (0019) 074, arXiv: 1810.00196 (cit. on p. 4).

[22] ATLAS Collaboration, *Luminosity determination in pp collisions at* $\sqrt{s} = 13$ *TeV using the ATLAS detector at the LHC*, ATLAS-CONF-2019-021 (2019), URL: https://cds.cern.ch/record/2677054 (cit. on p. 4).

[23] T. Gleisberg et al., *Event generation with SHERPA 1.1*, JHEP **02** (0009) 007, arXiv: 0811.4622 (cit. on p. 4).

[24] L. Hung-Liang et al., *New parton distributions for collider physics*, Phys. Rev. D **82** (2010) (cit. on p. 4).

[25] ATLAS Collaboration, *Search for new high-mass phenomena in the dilepton final state using 36* fb^{-1} *of proton-proton collision data at* $\sqrt{s} = 13$ *TeV with the ATLAS detector*, JHEP **10** (2017) 182, arXiv: 1707.02424 (cit. on p. 4).

[26] W. Verkerke and D. P. Kirkby, *The RooFit toolkit for data modeling*, eConf **C0303241** (2003) MOLT007, ed. by L. Lyons and M. Karagoz, arXiv: physics/0306116 (cit. on p. 4).

[27] ATLAS Collaboration, *Electron reconstruction and identification in the ATLAS experiment using the 2015 and 2016 LHC proton–proton collision data at* $\sqrt{s} = 13$ *TeV*, Eur. Phys. J. C **79** (2019) 639, arXiv: 1902.04655 (cit. on p. 5).

[28] ATLAS Collaboration, *Muon reconstruction performance of the ATLAS detector in proton–proton collision data at* $\sqrt{s}$ *=13 TeV*, Eur. Phys. J. C **76** (2016) 292, arXiv: 1603.05598 (cit. on p. 5).

[29] L. Moneta et al., *The RooStats Project*, PoS **ACAT2010** (2010) 057, ed. by T. Speer et al., arXiv: 1009.1003 (cit. on p. 9).

Appendices

A Limits using $\mathcal{F}$ scaling in cross-section

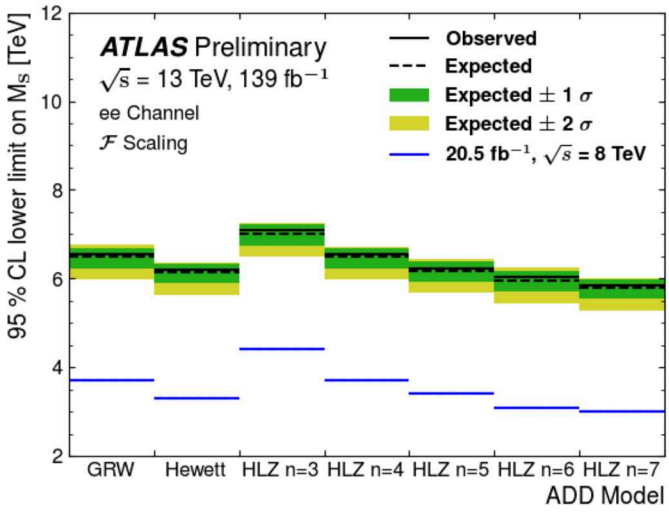

Figure 7: Lower limits, at 95% confidence level, on M_S in TeV for the ADD large extra dimensional model in the dielectron channel for different model conventions, scaling the cross section by $\mathcal{F}$.

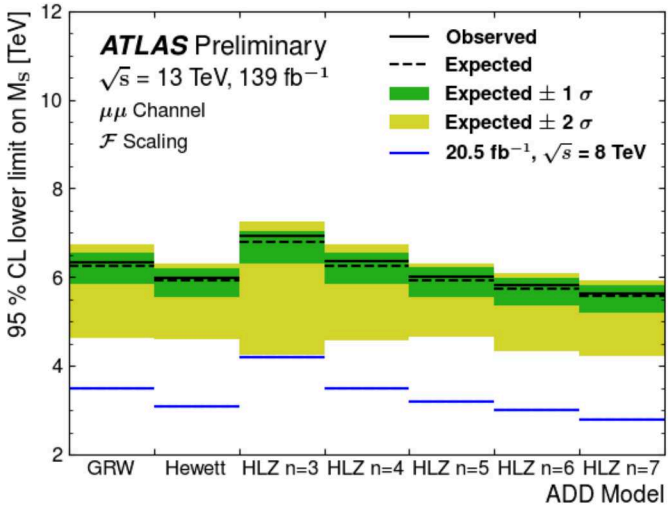

Figure 8: Lower limits, at 95% confidence level, on M_S in TeV for the ADD large extra dimensional model in the dimuon channel for different model conventions, scaling the cross section by $\mathcal{F}$.